

## DNA Triple-Helix Specific Intercalators As Antigene Enhancers: Unfused Aromatic Cations<sup>†</sup>

W. David Wilson,<sup>\*,‡</sup> Farial A. Tanious,<sup>‡</sup> Shaikh Mizan,<sup>‡</sup> Shijie Yao,<sup>‡</sup> Alexander S. Kiselyov,<sup>‡</sup> Gerald Zon,<sup>§</sup> and Lucjan Strekowski<sup>‡</sup>

Department of Chemistry and Laboratory for Chemical and Biological Sciences, Georgia State University, Atlanta, Georgia 30303, and Lynx Therapeutics, Incorporated, Foster City, California 94404

Received May 19, 1993; Revised Manuscript Received August 2, 1993\*

**ABSTRACT:** Triple-helical structures involving the interaction of an oligonucleotide third strand with a duplex nucleic acid sequence have recently gained attention as a therapeutic strategy in the "antigene" approach [cf. Helene, C. (1991) *Eur. J. Cancer* 27, 1466-1471]. This method utilizes the triple helix formed from the cellular duplex and an added third strand to directly regulate the activity of a selected gene. The limited stability of nucleic acid triple-helical interactions, particularly if the third strand has backbone modifications such as methylphosphonate or phosphorothioate substitutions, is a limiting condition for the use of this approach. We have designed and synthesized compounds, on the basis of the following three criteria, that we feel should provide selective interactions and significant stabilization of triplexes: appropriate aromatic surface area for stacking with triplex bases in an intercalation complex, positive charge, and limited torsional freedom in the aromatic system to match the propeller twist of the triple-base interactions in the triplex. A series of quinoline derivatives with an alkylamine side chain at the 4-position and with different aryl substituents at the 2-position has been synthesized as our first compounds. A 2-naphthyl derivative provides significant and selective stabilization of the triplex. In a 0.2 M NaCl buffer, the naphthyl derivative increased the  $T_m$  for the triplex (triplex to duplex and third strand transition) by approximately 30 °C more than the  $T_m$  increase for the duplex (duplex to single strands transition). Spectral changes and energy-transfer results indicate that the naphthyl compound and related derivatives bind to the triplex by intercalation. Molecular modeling results indicate very good stacking of the naphthylquinoline ring system with the bases at a triplex intercalation site, but the results also indicate that the ring system is too large to stack optimally with base pairs at a duplex intercalation site.

The triple-helix structure of nucleic acids with a third strand of pyrimidines forming hydrogen bonds with purines in a purine-pyrimidine duplex sequence Figure 1 was discovered shortly after the Watson-Crick model for the double helix (Felsenfeld et al., 1957; Felsenfeld & Miles, 1967). Individual triple-base interactions were observed in tRNA crystal structures (Saenger, 1984), but the possible biological roles of an extended triplex were expanded by the discovery of the H-DNA structure in natural DNA samples (Mirkin et al., 1987; Hanvey et al., 1988; Wells et al., 1988). H-DNA is an intramolecular triplex that is generally of the pyrimidine-purine-pyrimidine type and can be formed at mirror repeat sequences in supercoiled plasmids (Wells et al., 1988).

Various biotechnology applications have also led to an increased interest in triplex interactions. An oligomer, for example, can be used to bind specifically at a sequence in a long duplex DNA molecule through the formation of triple-base interactions (Helene, 1991a; Maher et al., 1992; Sun & Helene, 1993) and can be used to either manipulate enzymatic modifications of DNA (Strobel & Dervan, 1992) or devise triplex affinity capture schema (Ito et al., 1992; Takabatake et al., 1992). With appropriate cleaving groups attached to the third-strand oligomer, highly specific cleavage of DNA molecules as long as chromosomal DNA can be achieved (Moser & Dervan, 1987). The development of novel bases that increase the recognition possibilities of the third-strand oligonucleotide for duplex sequences can greatly expand the

range of application of these new capture probes or artificial nucleases (Ono et al., 1991; Griffin et al., 1992; Krawczyk et al., 1992; Froehler & Ricca, 1992; Stolz & Dervan, 1993; Sun & Helene, 1993).

The therapeutic potential of triplex interactions has also generated considerable excitement. Initial interest in nucleic acids as gene regulatory therapeutic agents focused on their potential to block translation through antisense interactions with mRNA (Zamecnik & Stephenson, 1978; Blake et al., 1985; Zon, 1988; Uhlmann & Peyman, 1990; Ts'o et al., 1992; Wickstrom, 1991). Since the number of mRNA transcripts can greatly outnumber the gene copies in a cell, there are some obvious advantages to the formation of a triplex to block transcription of the gene, i.e., the antigene strategy (Uhlmann & Peyman, 1990; Helene & Toulme, 1990; Helene, 1991b). Thus, in addition to the possible higher potency of triplex vs antisense drugs based on the difference in target numbers, the triplex approach provides means for rendering a specific gene dysfunctional by, for example, alkylation (Uhlmann & Peyman, 1990), which could be especially useful against integrated HIV-1, HBV, HCV, etc. Another unique feature is that, since triplex nucleic acid structures are rare in biological systems, targeting of secondary effector molecules or codrugs to triplexes can, in principle, be highly specific with the minimization of undesired side effects.

While there have been reports of antigene inhibitory effects against SV40 replication in CV-1 cells (Birg et al., 1990), IL2R $\alpha$  transcription in lymphocytes (Orson et al., 1991), C-myc transcription in HeLa cells (Postel et al., 1991), and HIV-1 in infected human cells (McShan et al., 1992), a

<sup>†</sup> This work was supported by NIH Grant AI-27196

<sup>‡</sup> Georgia State University.

<sup>§</sup> Lynx Therapeutics, Inc.

\* Abstract published in *Advance ACS Abstracts*, September 15, 1993.

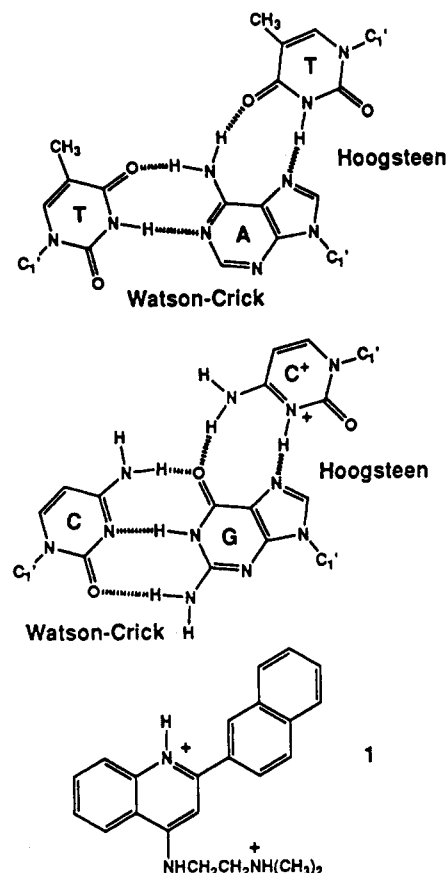


FIGURE 1: Base interactions for T·A·T and C<sup>+</sup>·G·C and the structure for 1.

recognized (Helene, 1991b; Maher et al., 1992; Mergny et al., 1992) limiting feature of antigene therapy is the relatively low stability of many triplexes. The C<sup>+</sup>·G·C triple helix has a protonated cytosine (Figure 1) which requires low pH for optimum formation. Because of the high charge density of triplex structures, they also require a significant cation concentration for stabilization (Cantor & Schimmel, 1980). Circumvention of these factors, which limit triplex stability under normal conditions, is being pursued along three primary lines: (i) design of modified bases that both increase the recognition possibilities and remove the requirement for protonation (Griffin et al., 1992; Stilz & Dervan, 1993; Krawczyk et al., 1992; Froehler & Ricca, 1992; Ono et al., 1991); (ii) backbone modifications that provide third-strand oligomer stability and can have reduced charge density and enhanced membrane permeability for cellular transport (Zon, 1988; Nielsen et al., 1991; Tso et al., 1992); and (iii) design of agents that specifically bind to the triplex assembly and significantly enhance the stability of the triplex relative to the corresponding duplex and single-stranded oligomer (Mergny et al., 1992).

Compared to the extensive database on the interaction of organic cations with duplex nucleic acids, relatively few studies have been conducted on triplex complexes with such reagents. Groove-binding agents such as netropsin (Breslauer & Park, 1992; Durand et al., 1992) and distamycin (S. Mizan and W. D. Wilson, unpublished results) generally destabilize the triplex relative to duplex structures. The prototype intercalator ethidium stabilizes T·A·T type triplexes (Scaria & Shafer, 1991), but can destabilize triplexes that contain C<sup>+</sup>·G·C triple base interactions (Mergny et al., 1991). Although the compounds described above generally destabilize triple helical structures, Helene and co-workers (Mergny et al., 1992)

recently discovered a heterocyclic intercalator that binds with high specificity to some triplex sequences and significantly stabilizes the triple helix relative to the corresponding duplex.

As part of our efforts to enhance the therapeutic applications of oligonucleotides, we are pursuing the design of compounds that provide specific stabilization of triplexes relative to duplexes. We have focused initially on intercalators since, at present, no good triplex groove-binding agents have been identified. Three essential features were included in our molecular design considerations: (i) the compounds should be cations to complement the high negative charge density of the triple helix; (ii) the compounds should have an aromatic surface area which optimally stacks with the three bases in the triplex; and (iii) the compounds should have an unfused aromatic system with torsional flexibility since the three bases in a triplex interaction have two contact points of torsional freedom (propeller twist). One of our first compounds that incorporates these structural features is shown in Figure 1, and we report here that it and related derivatives have very pronounced interaction selectivity for triplex relative to duplex structures. We also report that the compound markedly stabilizes triplexes which have third strands that are backbone-modified with phosphorothioates to affect both nuclease resistance *in vivo* (Agrawal et al., 1991; Bayever et al., 1992) and favorable cellular transport properties (Marti et al., 1992; Iversen et al., 1992; Gao et al., 1993). Extension to methylphosphonate analogs (Kibler-Herzog et al., 1990) has also been examined. Our studies to date have been with the T·A·T triplex, since this system forms a well-defined triplex with polymers and oligomers that does not require protonation. Future work will include triplexes with C<sup>+</sup>·G·C base interactions as well as purine-purine-pyrimidine triple-helical structures.

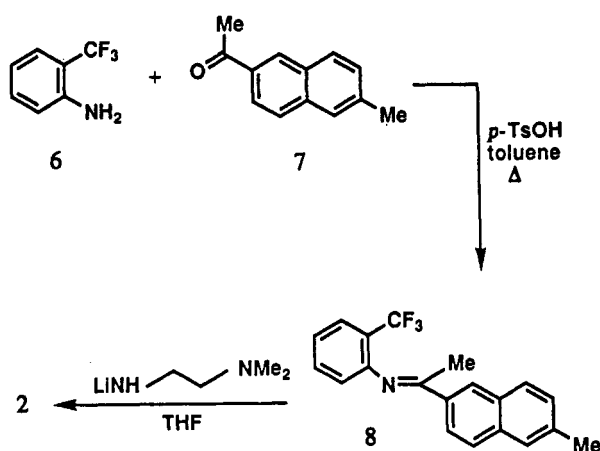
## MATERIALS AND METHODS

**Nucleic Acid Samples.** The nucleic acid oligomers dA<sub>19</sub>, dT<sub>19</sub>, and their methylphosphonate and phosphorothioate derivatives were synthesized, purified, and characterized as previously described (Kibler-Herzog et al., 1990, 1993). Poly(dA) and poly(dT) from Pharmacia were dissolved in PIPES 20 buffer [ $1 \times 10^{-2}$  M piperazine-*N,N'*-bis(2-ethanesulfonic acid),  $1 \times 10^{-3}$  M EDTA, and 200 mM NaCl adjusted to pH 7.0]. The concentrations of the polymer stock solutions were determined by using molar nucleotide extinction coefficients of  $8600 \text{ M}^{-1} \text{ cm}^{-1}$  at 257 nm for poly(dA) and  $8700 \text{ M}^{-1} \text{ cm}^{-1}$  at 265 nm for poly(dT) (Chamberlin, 1965). Poly(dA):poly(dT) 1:1 and 1:2 molar ratio mixtures were prepared by addition of the polymer stock solutions to 1 mL of PIPES 20 buffer. The samples were heated in a water bath to 90 °C and cooled slowly to room temperature to form the final complexes.

The preparations of quinolines 1 (Wilson et al., 1992), 3 and 4 (Strekowski et al., 1991), and 5 (Zhao et al., 1993) have been reported. The synthesis of 2 is outlined in Scheme I.

***N*-[2-(Dimethylamino)ethyl]-2-(6-methyl-2-naphthyl)-quinolin-4-ylamine (2).** Condensation of 2-(trifluoromethyl)-aniline (6) with 2-acetyl-6-methylnaphthalene (7) by using a general procedure (Strekowski et al., 1991, 1992) gave *N*-[1-(6-methyl-2-naphthyl)ethylidene]-2-(trifluoromethyl)-aniline (8): yield, 87%; mp 104.5–105 °C (from ethanol); <sup>1</sup>H NMR (CDCl<sub>3</sub>, 400 MHz)  $\delta$  2.26 (s, 3H), 2.52 (s, 3H), 6.81 (d, *J* = 7.1 Hz, 1H), 7.07 (t, *J* = 7.1 Hz, 1H), 7.50 (t, *J* = 7.1 Hz, 1H), 7.55 (m, 1H), 7.72 (d, *J* = 7.1 Hz, 1H), 7.88 (m, 1H), 7.94 (m, 1H), 7.98 (m, 1H), 8.20 (d, *J* = 7.1 Hz, 1H), 8.35 (s, 1H); MS *m/z* (relative intensity) 312 (100), 327

Scheme I



(42,  $M^+$ ). Anal. ( $C_{20}H_{16}F_3N$ ) C, H, N. Ketimine **8** was cyclized in the presence of lithium 2-(dimethylamino)-ethylamide by using a general procedure (Strekowski et al., 1991, 1992) to give **2**: yield, 57%; mp 186–186.5 °C (from acetone);  $^1H$  NMR ( $CDCl_3$ , 400 MHz)  $\delta$  2.33 (s, 6H), 2.54 (s, 3H), 2.74 (t,  $J = 5.7$  Hz, 2H), 3.43 (t,  $J = 5.7$  Hz, 2H), 5.92 (br s, exchangeable with  $D_2O$ , 1H), 6.99 (s, 1H), 7.34 (d,  $J = 7.3$  Hz, 1H), 7.43 (t,  $J = 5.8$  Hz, 1H), 7.65 (m, 2H), 7.81 (d,  $J = 5.8$  Hz, 1H), 7.87 (m, 1H), 7.88 (d,  $J = 7.3$  Hz, 1H), 8.10 (d,  $J = 7.3$  Hz, 1H), 8.25 (d,  $J = 7.3$  Hz, 1H), 8.52 (s, 1H); MS  $m/z$  (relative intensity) 58(100), 355(5,  $M^+$ ). Anal. ( $C_{24}H_{25}N_3$ ) C, H, N.

**$T_m$  Determinations and UV-Visible Spectra.** Thermal melting curves for DNA and complexes were determined as previously described (Kibler-Herzog et al., 1990, 1993). Both  $T_m$  measurements and UV-visible spectra were determined on a Varian Cary 4 spectrophotometer interfaced to a Dell/486 microcomputer. Absorption changes at 260 or 284 nm were followed as a function of temperature, and  $T_m$  values were determined from first derivative plots after the data was transferred to a Macintosh computer. Compounds are compared by the increase in  $T_m$  ( $\Delta T_m = T_m$  of the complex –  $T_m$  of the free nucleic acid) they produce in PIPES 20 buffer at saturating amounts of the compound (a ratio of 0.2 mol of compound to nucleic acid bases) unless otherwise indicated.

**Fluorescence Spectroscopy: Energy Transfer.** Fluorescence emission and excitation spectra were recorded on an SLM 8000 spectrofluorometer interfaced to an IBM computer. Fluorescence emission spectra were recorded from the edge of the scatter peak at 350 to 600 nm with excitation at 350 nm. Excitation spectra were recorded from 250 to 450 nm with an emission wavelength of 454 or 470 nm for either free compound ( $2 \times 10^{-7}$  M) or compound bound to the duplex or triplex.

Energy transfer from the polynucleotide to the bound compound was determined from the excitation and absorption spectra of the polynucleotide complex in the wavelength range 220–350 nm as previously described (Scaria & Shafer, 1991; Mergny et al., 1991, 1992). Similar results were obtained with emission wavelengths of 454 and 470 nm in excitation spectra. The energy transfer from the DNA bases to the bound compound is evaluated by the relative quantum yield ratios of the bound compound with excitation in the UV region normalized to excitation at 305 nm where DNA no longer

absorbs, according to the equation,

$$Q(UV)/Q(305) = [I(UV)_b/I(UV)_f][OD(UV)_f/OD(UV)_b]/[I(305)_b/I(305)_f][OD(305)_f/OD(305)_b]$$

where  $I$  and  $OD$  are, respectively, the measured fluorescence intensity and absorbance of free (f) and bound (b) compound at the same concentration.

**Molecular Modeling.** A triplex DNA structure,  $dT_{10} \cdot dA_{10} \cdot dT_{10}$ , was generated with fiber diffraction triple-base coordinates (Arnott et al., 1976) and crystal symmetry operations in the Tripos SYBYL 6.0 molecular modeling package. The structure was prepared with terminal 5'- and 3'-OH groups and was minimized. Calculations according to the ion condensation theory for polyelectrolytes (Manning, 1978) indicate that a net charge of –0.15 esu per nucleotide is expected for triple-helix DNA with a linear phosphate spacing of  $(3.4/3) = 1.13$  Å. To distribute –0.15 esu charge over the nucleotide unit, ab initio calculations with the Spartan 4.0 software package and an STO-3G basis set were performed on dimethyl phosphate with a net charge of either –1 or 0 esu. Interpolations were then made between the two sets of values to obtain a scaling factor to give the desired –0.15 esu charge on the nucleotide. The final point charge on phosphorus is 1.68 esu, on each of the two ester oxygens is –0.505 esu, and on each of the other two phosphate oxygens is –0.575 esu, and the remaining atoms of the nucleotide contribute a net positive charge of +0.33 esu (Weiner et al., 1986) to provide a total final change of –0.15 esu per nucleotide. Because the intercalators studied in this work are dications, an additional +1.70 esu of charge was distributed on the nucleotides at the intercalation site as described above to mimic counterion release (Veal & Wilson, 1991).

The general intercalation site geometry was based on crystal structures such as the ethidium complex with dinucleotides (Jain & Sobell, 1984), and an intercalation site was generated at the center of the minimized 10-base triple segment by using previously described methods (Veal & Wilson, 1991; Yao & Wilson, 1992). Distance and torsional constraints were applied to the two central base triples at the intercalation site, and the hydrogen bonds of both the Watson–Crick and the Hoogsteen base interactions were maintained by distance constraints during energy minimization to create the intercalation site.

As in previous work (Veal & Wilson, 1991), the point charges of the intercalators were calculated with the AM1 molecular orbital program in SYBYL. The intercalator structures were energy refined and then manually docked into the triplex intercalation site in several orientations that gave excellent base–intercalator stacking with no significant unfavorable van der Waals interactions. The potential energy equation defined by Kollman and co-workers (Weiner et al., 1986) and a modified version (Veal & Wilson, 1991) of the Kollman all-atom force field were used to energy-minimize these complexes. Molecular mechanics calculations were performed using the Tripos SYBYL molecular modeling package on either Silicon Graphics Iris or Indigo workstations. In all calculations, an RMS gradient of 0.08 kcal/mol·Å<sup>2</sup> was chosen as the convergence criterion, and a distance-dependent dielectric constant of the form  $\epsilon = 4r_{ij}$  was used.

## RESULTS

**Unmodified DNA Triplexes.** Triplex to duplex and single strand transitions [ $(dT_n \cdot dA_n \cdot dT_n)$  to  $(dT_n + dA_n \cdot dT_n)$ ] at low temperature followed by duplex denaturation transitions at higher temperature are well-resolved in 0.2 M NaCl buffer for both polymers and oligomers 19 nucleotides long (oligomer

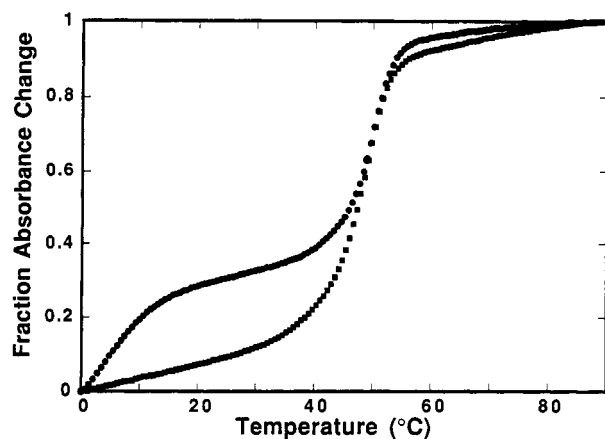


FIGURE 2: Absorbance changes at 260 nm as a function of temperature for  $dA_{19} \cdot dT_{19}$  (■) and  $dT_{19} \cdot dA_{19} \cdot dT_{19}$  (●) in PIPES buffer with 0.2 M NaCl. At 284 nm (not shown), the low-temperature transition has a much larger relative amplitude.

transitions are shown in Figure 2). Assignment of the low-temperature transition to the triplex to duplex dissociation is supported by an independent analysis of the duplex denaturation (Figure 2) and by monitoring the transitions at 284 nm where the triplex to duplex dissociation has much larger absorption changes than duplex denaturation (Riley et al., 1966). This assignment of triplex and duplex transitions is also in agreement with earlier studies on pyrimidine-purine-pyrimidine triplexes [cf. Cantor and Schimmel (1980)]. At salt concentrations below 0.2 M NaCl, the triplex transition cannot be seen for the oligomer, and at NaCl concentrations near 1 M, the triplex and duplex transitions approach a common  $T_m$  value. Cooling the denatured oligomer samples under these conditions at a rate of 0.5 °C/min gave reversible behavior with no significant hysteresis.

**Modifications on the Third Strand.** With the  $dA_{19} \cdot 2dT_{19}$  oligomer triplex we have investigated the effects on triplex stability of a third strand modified with either methylphosphonate linkages ( $dT^*_{19}$  which has 17 methylphosphonate linkages and a normal phosphodiester at the 5'-end) or phosphorothioate linkages ( $dTS_{19}$  which has all 18 phosphorothioate linkages). In agreement with previous results, we find with methylphosphonate (Kibler-Herzog et al., 1990) or phosphorothioate (L. Kibler-Herzog, G. Zon, and W. D. Wilson, unpublished results) linkages in the third strand that no triplex transition is observed up to 1 M NaCl. The transition for the normal duplex ( $dA_{19} \cdot dT_{19}$ ) in these mixtures is seen at all salt concentrations. When the oligomers have a third strand with alternating modified (either methylphosphonate or phosphorothioate) and normal phosphodiester groups, triplex transitions between 0 and 10 °C are observed at 0.5 M NaCl (not shown), but no triplex transition is seen at 0.2 M NaCl as in Figure 2. The normal duplex denaturation is seen at high temperature in all of these experiments.

**Triplex-Ligand Interactions.** The  $dA_{19} \cdot dT_{19}$  duplex can be selectively stabilized by intercalators as shown in Figure 3A. The intercalators propidium and naphthylquinoline **1** have relatively small effects on the duplex  $T_m$  at this salt concentration, but the AT-specific minor groove-binding antibiotic netropsin markedly stabilizes the duplex. All of these compounds cause significantly larger increases in the duplex  $T_m$  at lower salt concentrations. Results with the  $dT_{19} \cdot dA_{19} \cdot dT_{19}$  triplex are significantly different from the duplex results (Figure 3B). Netropsin destabilizes the triplex to duplex transition, and the dissociation occurs below 0 °C under these conditions in the presence of netropsin. Propidium

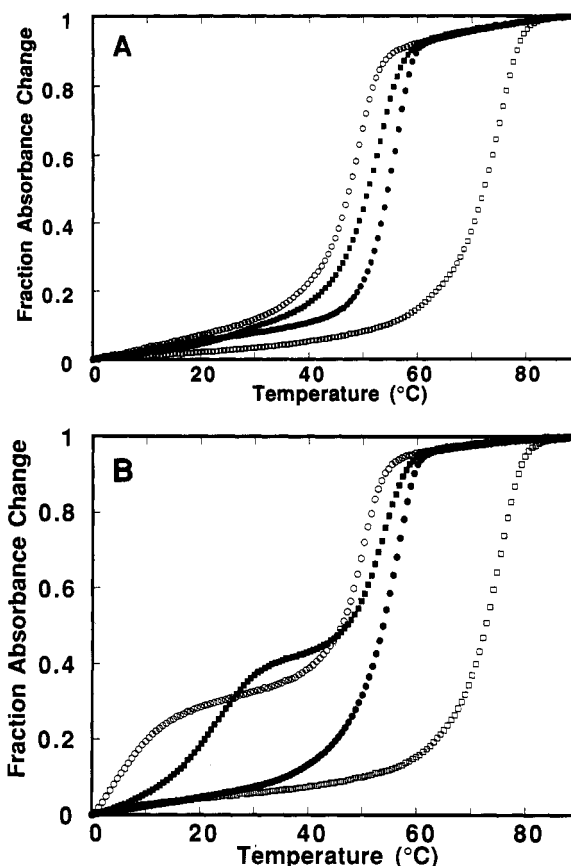


FIGURE 3: Melting curves at 260 nm for (A)  $dA_{19} \cdot dT_{19}$  or (B)  $dT_{19} \cdot dA_{19} \cdot dT_{19}$  (○) and complexes with propidium (■), **1** (●), and netropsin (□) in PIPES buffer with 0.2 M NaCl. The ratio of compound to dA bases in the nucleic acid is 0.2. The  $\Delta T_m$  values in A are as follows: propidium, 4.3; **1**, 7.1; netropsin, 26. The  $\Delta T_m$  values in B for the duplex (high temperature transition) are as follows: propidium, 4.5; **1**, 7.0; netropsin, 25.2. For the triplex (lower temperature transition): propidium, 22.3; **1**, 56.4; netropsin, <0.

stabilizes the triplex more than the duplex, but the increase in  $T_m$  for the triplex to duplex transition is still relatively small. The quinoline intercalator, **1**, provides very selective stabilization of the triple-helical species (Figure 3B). At a ratio of 0.2 mol of **1**/mol of  $dA_{19}$  in the triplex, the transition for triple helix to double helix and single strand has merged with the duplex denaturation, and the only observed transition is for triplex to three single strands. At lower ratios of **1**, the triplex transition can be observed as a separate curve at temperatures below the duplex transition.

Stabilization of triplexes having modified third strands (Figure 4) is even more dramatic than that observed with the unmodified oligomers. At 0.2 M NaCl, no triplex transition is observed with the  $dTS_{19}$  third strand. Addition of netropsin stabilizes the duplex in the normal fashion, but no triplex transition is observed. On addition of propidium, a broad triplex transition, centered near 10–15 °C, is observed. With quinoline **1**, on the other hand, a very marked stabilization of the triplex occurs, and the triplex transition appears as a shoulder on the duplex transition under these conditions. This represents an enormous stabilization of the triplex, from a  $T_m$  below 0 to near 40 °C.

Results for the methylphosphonate third strand are less clear (Figure 4B). As expected, no triplex transition is seen in the presence of netropsin or for the system without added compounds. A small hump on the base line at low temperature in the presence of propidium suggests a limited triplex transition. With **1** a broad, very low cooperativity transition

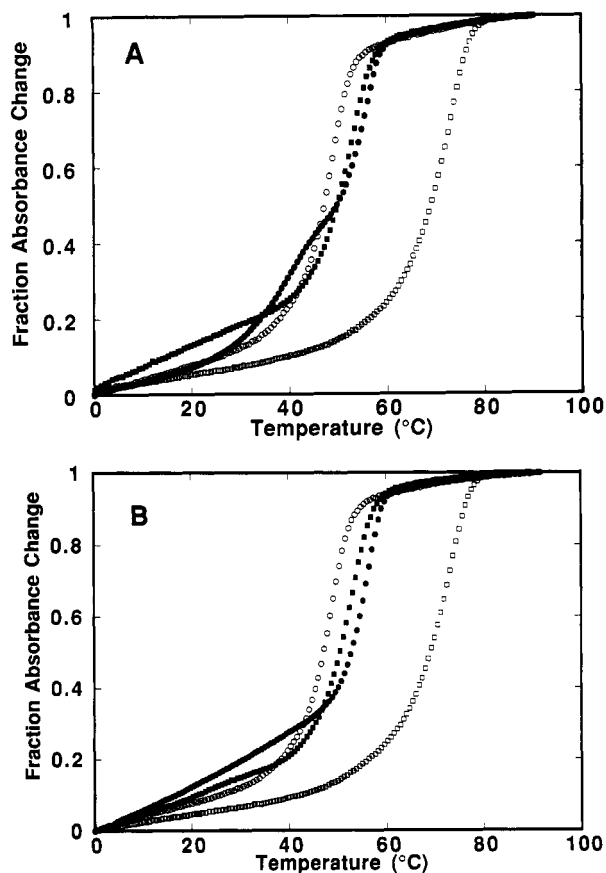


FIGURE 4: Melting curves at 260 nm for (A) dT<sub>19</sub>-dA<sub>19</sub>-dTS<sub>19</sub> or (B) dT<sub>19</sub>-dA<sub>19</sub>-dT\*<sub>19</sub> (O) and complexes with propidium (■), 1 (●), and netropsin (□) in PIPES buffer with 0.2 M NaCl. The ratio of compound to dA bases in the nucleic acid is 0.2.

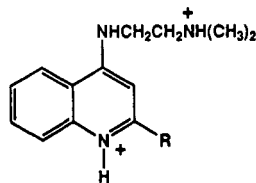
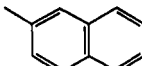
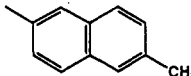
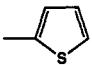
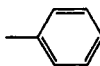
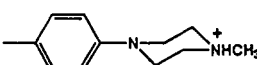
is observed at low temperature, but it is clear that the population of isomers in the methylphosphonate sample has a larger effect on the triplex stability and transition breadth than is observed with a third-strand phosphorothioate.

**Binding Mode.** Ethidium (Scaria & Shafer, 1991; Mergny et al., 1991) and the pyridoindole aromatic cation studied by the Helene group (Mergny et al., 1992) intercalate into triplex conformations. The structure of naphthylquinoline 1 (Figure 1) suggests that it should also bind most strongly by intercalation. Energy-transfer studies (not shown), conducted as described for other triplexes (Scaria & Shafer, 1991; Mergny et al., 1992), indicate significant energy transfer from the bases of the triplex to the aromatic system of 1, confirming an intercalative binding mode with the triplex for this compound.

**Similar Additional Unfused Aromatic Quinoline Dications.** Several additional quinoline derivatives have been evaluated for their ability to selectively stabilize polymer triplex conformations (Table I). None of the compounds binds very strongly to the duplex under these conditions, but their interactions with the triplex vary widely. The interaction with the triplex drops markedly if the naphthyl substituent is replaced by a smaller phenyl (4) or thiophene (3) ring (Table I).

Addition of a cationic piperazyl substituent to the phenyl ring to give 5 results in a large increase in the  $T_m$  of the triplex transition. Of these quinoline derivatives, the naphthyl derivative, 1, has the largest  $\Delta T_m$  for the triplex transition, and methyl substitution on the naphthyl ring (2) slightly decreases the  $\Delta T_m$  value for the triplex and duplex (Table I).

Table I:  $T_m$  Increases for Polymer Duplex and Triplex Structures with the Quinoline Derivatives<sup>a</sup>

			
compound	R	$\Delta T_m$ duplex	$\Delta T_m$ triplex
1		5.5	35.6
2		2.2	32.9
3		0.7	9.4
4		0.3	11.9
5		2.2	27.3

<sup>a</sup> The free duplex, poly(dA-dT), has a  $T_m$  of 74.1 °C, and the triplex transition is at 43.8 °C for dT-dA-dT under these conditions.

Table II: Intermolecular Energy Terms for Intercalators That Bind to the dT<sub>10</sub>-dA<sub>10</sub>-dT<sub>10</sub> Model Triplex<sup>a</sup>

complex <sup>b</sup>	$E_{vdW}$	$E_{ES}$	$E_{HB}$	$E_{total}$
4-TAT	-49.77	-9.23	-0.06	-59.06
core structure	-31.99	-7.93	-0.06	-39.98
phenyl	-17.78	-1.30	0.00	-19.08
1-TAT	-57.69	-9.22	-0.07	-66.98
core structure	-31.36	-7.93	-0.07	-39.36
naphthyl	-26.33	-1.29	0.00	-27.62

<sup>a</sup> Energies are in kilocalories/mole.  $E_{vdW}$  = van der Waals interaction energy;  $E_{ES}$  = electrostatic interaction energy;  $E_{HB}$  = hydrogen-bonding interaction energy;  $E_{total} = E_{vdW} + E_{ES} + E_{HB}$ . Interaction energies are calculated by taking the DNA triplex and intercalator as two different aggregates in the complex. The difference between the calculated energies of the aggregates in the minimized complex gives the interaction energies.

<sup>b</sup> The core structure consists of the quinoline ring system and alkylamine side chain, which is common to all of the derivatives.

**Molecular Modeling.** The naphthylquinoline 1 was docked into the intercalation site generated in the center of a dT<sub>10</sub>-dA<sub>10</sub>-dT<sub>10</sub> oligomer triplex in several different orientations, as described in the Materials and Methods section, and the energy was minimized. Low-energy complexes were obtained with the side chain docked into both the minor groove and the large major groove. Complexes with the side chain in the minor groove have slightly better interaction energies. The minor groove complex with the lowest energy is shown in Figure 5 with a top view in Figure 6. The orientations of the compound and the DNA base triples are as shown schematically in Figure 1. As can be seen from these figures, the quinoline and naphthyl aromatic rings form an excellent stacked complex with the bases at the intercalation site. For comparison purposes, the phenyl derivative 4 was docked into a similar initial complex, and the complex energy was minimized in the same way as for 1 (Figures 5 and 6 show corresponding views of the two complexes). The cationic side chains and quinoline rings of the two complexes have similar orientations, but the naphthyl ring forms a much better stacking interaction with the thymine bases in the third strand

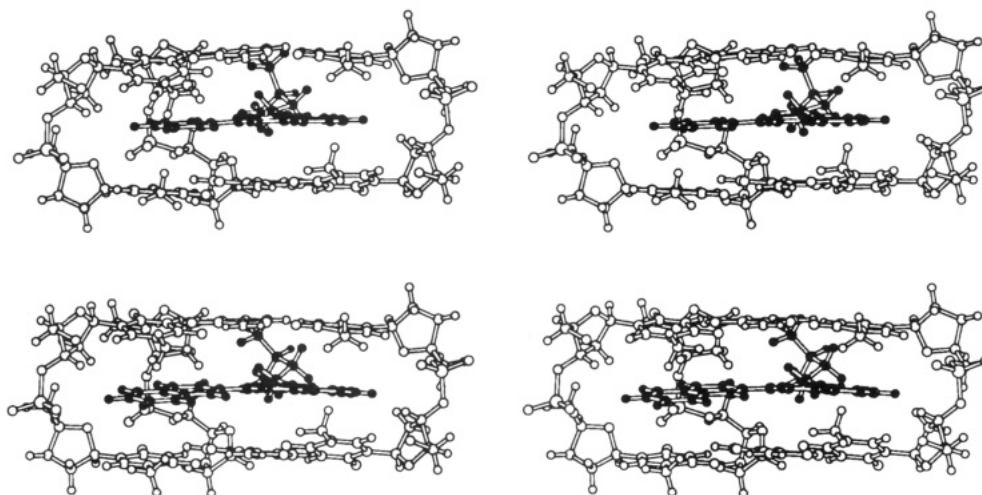


FIGURE 5: Stereoviews into the major groove of the central two base triples in the intercalation complexes of **1** (bottom) and **4** (top) with dT<sub>10</sub>-dA<sub>10</sub>-dT<sub>10</sub>. DNA is shown with open atoms and bonds, while the compounds have black atoms and open bonds. As can be seen in the figure, the quinoline and phenyl rings have close to a planar conformation in the **4** complex, while the quinoline and naphthyl rings have significant propeller twist in the **1** complex. The alkylamine side chain is in the minor groove at the rear of the structures as shown.

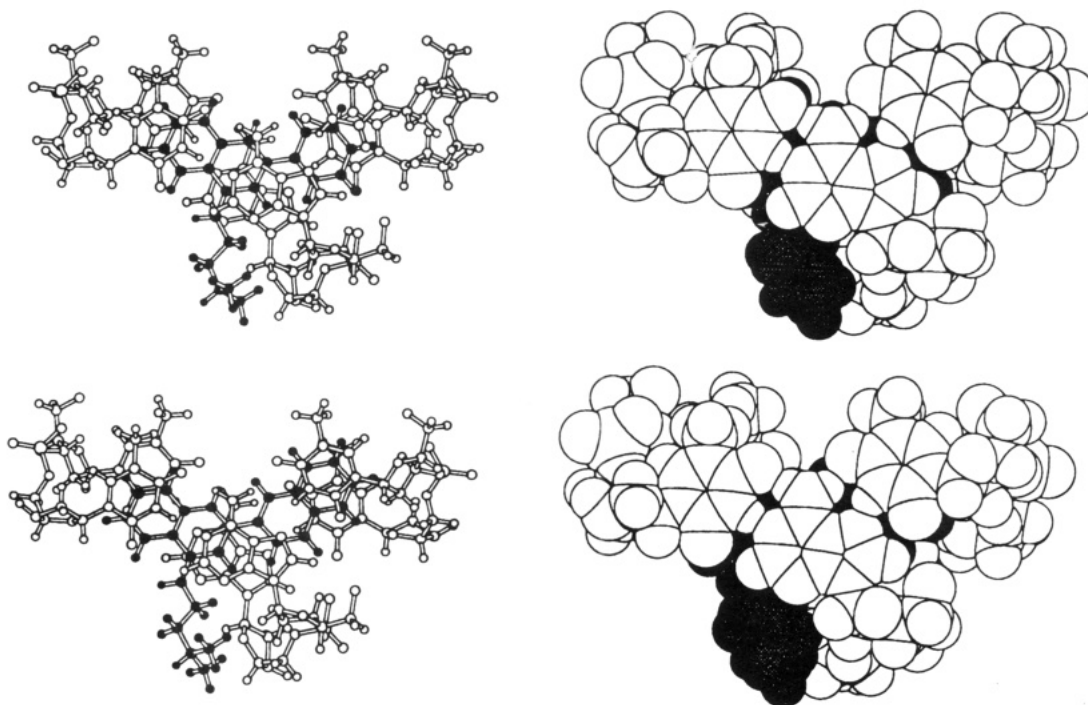


FIGURE 6: Top views of the models from Figure 5 are shown as stick drawings (left) or CPK models (right). The complex with **1** is at the bottom of the figure and the complex with **4** is at the top. The alkylamine side chains are in the minor groove and point to the bottom of the figure. The significantly better overlap of the naphthyl relative to the phenyl ring can be seen clearly in the views.

at the intercalation site than the smaller phenyl ring.

The intermolecular interaction energy terms between the bound intercalators and the triplex for the complexes in Figures 5 and 6 are collected in Table II. The electrostatic and hydrogen-bonding interaction energy terms are equivalent for the naphthyl and phenyl complexes. As expected, the van der Waals term for the interaction is significantly more favorable for the naphthyl than for the phenyl derivative, and the extra binding energy is localized almost exclusively on the naphthyl ring itself.

## DISCUSSION

It is generally recognized that the sugar-phosphate backbone must be modified to increase nuclease resistance and/or enhance membrane permeability when nucleic acids are used

in either the antisense or the antigene therapeutic strategy in biological systems. Two of the most extensively studied backbone modifications, methylphosphonates (Ts'o et al., 1992) and phosphorothioates (Zon, 1988; Zon & Stec, 1991b), the latter of which has exhibited antisense activity in animal models of several human diseases (Simons et al., 1992; Ratajczak et al., 1992; Offensperger et al., 1993), decrease triplex stability when targeted as the third strand of the T·A·T triplex motif (Figure 3). It is essential not only to regain but to enhance this stability if the antigene therapy concept is to be realized with these backbone modifications, especially for phosphorothioates, which are already in early phase human clinical trials involving genital warts (Cowsert et al., 1993) and acute myelogenous leukemia/myelodysplastic syndrome (Bayever et al., 1992; E. Bayever, personal communication). A method to enhance selectively the stability of nucleic acid



triplexes is to design cationic intercalators which display a pronounced binding preference for triplex over duplex motifs and which significantly enhance triplex stability. Since triplex nucleic acids are rare in biological systems, this approach can also provide highly directed targeting of the intercalators, whether attached or not to the third-strand oligomer.

Our initial criteria for the design of triplex-specific ligands are presented above, and a set of initial compounds for testing is shown in Table I. Figure 1 illustrates the rationale for the selection of **1** and derivatives as our first compounds for triplex interaction specificity: the stacking surface, rotational freedom, and charge of **1** are complementary to the triple-base structure. It is clear from the results in Table I that both positive charge and increased stacking surface enhance the triplex interaction strength and specificity of the quinoline derivatives. The phenyl- (**4**) and thiophene-substituted (**3**) compounds (Table I) cause increases in the polymer triplex to duplex transition temperature of approximately 10 °C, while the naphthyl- (**1**) and tricationic piperazylphenyl-substituted (**5**) compounds cause  $T_m$  increases of approximately 30 °C. These observations are in accord with the larger stacking surface of the bases in a triplex and the higher charge density of the triplex relative to the duplex.

The three cationic groups of **5** are spatially separated as are the backbone strands of the triplex, and the enhancement of the triplex stability by **5** suggests that the piperazyl substituent is in a good position to interact with at least one of the DNA backbone strands. The highest accessible anionic charge density in the triplex is in the remaining space of the large major groove, and preliminary molecular modeling studies suggest that the optimum bound conformation of **5** is with the piperazyl substituent in the major groove, the alkylamine cationic group in the minor groove, and the phenylquinoline aromatic system stacked with the bases of the triplex, much as shown for the phenyl derivative in Figures 5 and 6. Although **5** alone may not have sufficient membrane-transport characteristics for its use in antigene therapy, it could be covalently linked to an oligomer chain through either the piperazyl or alkylamine substituents, and it is of long-term interest because of this feature.

The naphthyl derivative should have good membrane-transport characteristics and is of immediate interest as an auxiliary agent in the antigene therapy approach. Structural characteristics and energy-transfer experiments clearly indicate that the naphthyl compound binds to the triplex by intercalation, as observed with ethidium (Scaria & Shafer, 1991; Mergny et al., 1991) and a pyridoindole heterocycle studied by Helene and co-workers (Mergny et al., 1992). Addition of a methyl group to the naphthyl ring in **2** causes a slight decrease in the triplex  $\Delta T_m$ , but the fractional  $\Delta T_m$  decrease for the duplex is larger, and **2** displays both strong triplex binding and a larger selectivity for triplex over duplex interactions than **1**. It is clear that we have much to learn about the effects of substituents on the nucleic acid interactions, and additional compounds to expand our understanding in this area are being designed and synthesized in our laboratories.

Molecular modeling experiments provide an explanation for the significantly enhanced stabilization of the triplex relative to duplex structure for these compounds. Both the quinoline and naphthyl rings of **1** are stacked over bases in the low-energy complex with the triplex (Figure 6), but part of the naphthyl ring protrudes from the base-pair stack in the low-energy complex with DNA duplexes (not shown). The corresponding derivative with a phenyl in place of the naphthyl ring system provides much less discrimination between the

triplex and duplex structures (Table I). The quinoline and the phenyl rings in **4** are well stacked with the duplex and triplex bases. The increased  $T_m$  of the triplex relative to the duplex with **4** probably arises in part due to the more favorable ionic effects of **4** with the more anionic triplex and partly due to improved van der Waals interactions of the aromatic system of **4** with the larger aromatic surface area in a triplex intercalation site.

One of the most exciting features of the naphthyl derivative is its ability to strongly stabilize triplexes with backbone-modified third strands, particularly phosphorothioates. As we have noted previously, methylphosphonate (Kibler-Herzog et al., 1990) and phosphorothioate (L. Kibler-Herzog, G. Zon, and W. D. Wilson, manuscript in preparation) modifications on the dT strand destabilize T-A-T type triplexes. Significant stabilization of methylphosphonate-substituted triplexes is obtained with **1**, but the transition curves are very broad. The stabilizing effects with phosphorothioate modifications are more pronounced and sharp transition curves are obtained. The anionic charge normally dispersed on the oxygens of a phosphate group appears to be more strongly localized on the sulfur atom of a phosphorothioate (Zon & Geiser, 1991a; Bergot & Egan, 1992), and this may account for the particularly strong interactions of **1** with the phosphorothioate-substituted triplex.

Both the methylphosphonate and phosphorothioate oligomer strands used to form the heterotriplexes are random diastereomeric mixtures having either  $R_p$  or  $S_p$  configurations at each substituted linkage. It is not clear why the methylphosphonate triplex gives such broad transitions while the phosphorothioate triplex gives a sharp transition curve, indicating that all isomeric complexes have similar and very high stability. As additional structural details emerge for triplex motifs, possible explanations for the molecular basis for these pronounced differences should arise. We are preparing additional unfused aromatic cations to probe the recognition requirements of DNA triplexes in more detail, and we plan to investigate the properties and applications of these triplex-specific intercalators when linked to phosphorothioate and other types of nuclease-resistant oligonucleotide analogs.

## REFERENCES

- Agrawal, S., Temsamani, J., & Tang, J. Y. (1991) *Proc. Natl. Acad. Sci. U.S.A.* **88**, 7595-7599.
- Arnott, S., Bond, P. J., Selsing, E., & Smith, P. J. C. (1976) *Nucleic Acids Res.* **3**, 2459-2470.
- Bayever, E., Iversen, P., Smith, L., Spinolo, J., & Zon, G. (1992) *Antisense Res. Dev.* **2**, 109-110.
- Bergot, B. J., & Egan, W. (1992) *J. Chromatogr.* **599**, 35-42.
- Birg, F., Praseuth, D., Zerial, A., Thuong, N. T., Asseline, U., Le Doan, T., & Helene, C. (1990) *Nucleic Acids Res.* **18**, 2901-2907.
- Blake, K. R., Murakami, A., Spitz, S. A., Glave, S. A., Reddy, M. P., Ts'o, P. O. P., & Miller, P. S. (1985) *Biochemistry* **24**, 6139-6145.
- Breslauer, K. J., & Park, Y.-W. (1992) *Proc. Natl. Acad. Sci. U.S.A.* **89**, 6653-6657.
- Cantor, C. R., & Schimmel, P. R. (1980) *Nucleic Acid Structural Transitions*, Chapter 2, W. H. Freeman and Company, New York.
- Chamberlin, M. J. (1965) *Fed. Proc.* **24**, 1446-1457.
- Cowser, L. M., Fox, M. C., Zon, G., & Mirabelli, C. K. (1993) *Antimicrob. Agents Chemother.* **37**, 171-177.
- Durand, M., Thuong, N. T., & Maurizot, J. C. (1992) *J. Biol. Chem.* **267**, 24394-24399.
- Felsenfeld, G., & Miles, H. T. (1967) *Annu. Rev. Biochem.* **36**, 407-448.

- Felsenfeld, G. D., Davies, D. R., & Rich, A. (1957) *J. Am. Chem. Soc.* 79, 2023–2024.
- Froehler, B. C., & Ricca, D. J. (1992) *J. Am. Chem. Soc.* 114, 8320–8322.
- Gao, W.-Y., Storm, C., Egan, W., & Cheng, Y.-C. (1993) *Mol. Pharmacol.* 43, 45–50.
- Giovannangeli, C., Rougee, M., Garesier, T., Thuong, N. T., & Helene, C. (1992) *Proc. Natl. Acad. Sci. U.S.A.* 89, 8631–8635.
- Griffin, L. C., Kiessling, L. L., Beal, P. A., Gillespie, P., & Dervan, P. B. (1992) *J. Am. Chem. Soc.* 114, 7976–7982.
- Hanvey, J. C., Shimizu, M., & Wells, R. D. (1988) *Proc. Natl. Acad. Sci. U.S.A.* 85, 6292–6296.
- Helene, C. (1991a) *Anti-Cancer Drug Des.* 6, 569–584.
- Helene, C. (1991b) *Eur. J. Cancer* 27, 1466–1471.
- Helene, C., & Toulme, J. J. (1990) *Biochim. Biophys. Acta* 1049, 99–125.
- Ito, T., Smith, C. L., & Cantor, C. R. (1992) *Nucleic Acids Res.* 20, 3524.
- Iversen, P. L., Zhu, S., Meyer, A., & Zon, G. (1992) *Antisense Res. Dev.* 2, 211–222.
- Jain, S. C., & Sobell, H. M. (1984) *J. Biomol. Struct. Dyn.* 1, 1179–1194.
- Kibler-Herzog, L., Kell, B., Zon, G., Shinozuka, K., Mizan, S., & Wilson, W. D. (1990) *Nucleic Acids Res.* 18, 3545–3555.
- Kibler-Herzog, L., Zon, G., Whittier, G., Mizan, S., & Wilson, W. D. (1993) *Anti-Cancer Drug Des.* 8, 65–79.
- Krawczyk, S. H., Mulligan, J. F., Wadwani, S., Moulds, C., Froehler, B. C., & Matteucci, M. D. (1992) *Proc. Natl. Acad. Sci. U.S.A.* 89, 3761–3764.
- Maher, L. J., III, Wold, B., & Dervan, P. B. (1989) *Science* 245, 725–730.
- Maher, L. J., III, Dervan, P. B., & Wold, B. (1992) *Biochemistry* 31, 70–81.
- Manning, G. S. (1978) *Q. Rev. Biophys.* 11, 179–246.
- Marti, G., Egan, W., Noguchi, P., Zon, G., Matsukra, M., & Broder, S. (1992) *Antisense Res. Dev.* 2, 27–39.
- McShan, W. M., Rossen, R. D., Laughter, A. H., Trial, J., Kessler, D. J., Zendegui, J. G., Hogan, M. E., & Orson, F. M. (1992) *J. Biol. Chem.* 267, 5712–5721.
- Mergny, J.-L., Collier, D., Rougee, M., Montenay-Garestier, T., & Helene, C. (1991) *Nucleic Acids Res.* 19, 1521–1526.
- Mergny, J. L., Duval-Valentin, G., Nguyen, C. H., Perrouault, L., Faucon, B., Rougee, M., Montenay-Garestier, T., Bisagni, E., & Helene, C. (1992) *Science* 256, 1681–1684.
- Mirkin, S. M., Lyamichev, V. I., Drushlyak, K. N., Dobrynin, V. N., Filippov, S. A., & Frank-Kamenetskii, M. D. (1987) *Nature* 330, 495–497.
- Moser, H. E., & Dervan, P. B. (1987) *Science* 238, 645–650.
- Nielsen, P. E., Egholm, M., Berg, R. H., & Buchardt, O. (1991) *Science* 254, 1497–1500.
- Offensperger, W.-B., Offensperger, S., Walter, G., Teubner, K., Iolol, G., Blum, H. E., & Gerok, W. (1993) *EMBO J.* 12, 1257–1262.
- Ono, A., Ts'o, P. O. P., & Kan, L.-S. (1991) *J. Am. Chem. Soc.* 113, 4032–4033.
- Orson, F. M., Thomas, D. W., McShan, W. M., Kessler, D. J., & Hogan, M. E. (1991) *Nucleic Acids Res.* 19, 3435–3441.
- Park, Y.-W., & Breslauer, K. J. (1992) *Proc. Natl. Acad. Sci. U.S.A.* 89, 6653–6657.
- Postel, E. H., Flint, S. J., Kessler, D. J., & Hogan, M. E. (1991) *Proc. Natl. Acad. Sci. U.S.A.* 88, 8227–8231.
- Ratajczak, M. Z., Kant, J. A., Luger, S. M., Zhang, J., Zon, G., & Gewirtz, A. M. (1992) *Proc. Natl. Acad. Sci. U.S.A.* 89, 1823–1827.
- Record, M. T., Anderson, C. F., & Lohman, T. M. (1978) *Q. Rev. Biophys.* 11, 103–178.
- Riley, M., Maling, B., & Chamberlin, M. J. (1966) *J. Mol. Biol.* 20, 359–389.
- Saenger, W. (1984) *tRNA—A Treasury of Stereochemical Information*, Springer-Verlag, New York.
- Scaria, P. V., & Shafer, R. H. (1991) *J. Biol. Chem.* 266, 5417–5423.
- Simons, M., Edelman, E. R., DeKeyser, J. L., Langer, R., & Rosenberg, R. D. (1992) *Nature* 359, 67.
- Stilz, H. U., & Dervan, P. B. (1993) *Biochemistry* 32, 2177–2185.
- Strekowski, L., Mokrosz, J. L., Honkan, V. A., Czarny, A., Cegla, M. T., Wydra, R. L., Patterson, S. E., & Schinazi, R. F. (1991) *J. Med. Chem.* 34, 1739–1746.
- Strekowski, L., Patterson, S. E., Janda, L., Wydra, R. L., Harden, D. B., Lipowska, M., & Cegla, M. T. (1992) *J. Org. Chem.* 57, 196–201.
- Strobel, S. A., & Dervan, P. B. (1992) *Triple Helix-Mediated Single-Site Enzymatic Cleavage of Megabase Genomic DNA*, Academic Press, Inc.
- Sun, J.-S., & Helene, C. (1993) *Curr. Opin. Struct. Biol.* 3, 345–356.
- Takabatake, T., Asada, K., Uchimura, Y., Ohdate, M., & Kusukawa, N. (1992) *Nucleic Acids Res.* 20, 5853–5854.
- Ts'o, P. O. P., Aurelian, L., Chang, E., & Miller, P. S. (1992) *Ann. N. Y. Acad. Sci.* 660, 159–177.
- Uhlmann, E., & Peyman, A. (1990) *Chem. Rev.* 90, 543–584.
- Veal, J. M., & Wilson, W. D. (1991) *J. Biomol. Struct. Dyn.* 8, 1119–1145.
- Weiner, S. J., Kollman, P. A., Nguyen, D. T., & Case, D. A. (1986) *J. Comput. Chem.* 7, 230.
- Wells, R. D., Collier, D. A., Hanvey, J. C., Shimizu, M., & Wohlrab, F. (1988) *FASEB J.* 2, 2939–2949.
- Wilson, W. D., Zhao, M., Patterson, S. E., Wydra, R. L., Janda, L., Streckowski, L., & Schinazi, R. F. (1992) *Med. Chem. Res.* 2, 102–110.
- Yao, S., & Wilson, W. D. (1992) *J. Biomol. Struct. Dyn.* 10, 367–387.
- Zamecnik, P. C., & Stephenson, M. L. (1978) *Proc. Natl. Acad. Sci. U.S.A.* 75, 280–284.
- Zhao, M., Janda, L., Nguyen, J., Streckowski, L., & Wilson, W. D. (1993) *Biopolymers* (in press).
- Zon, G. (1988) *Pharm. Res.* 5, 539–548.
- Zon, G., & Geiser, T. G. (1991) *Nucleic Acids Res.* 6, 539–568.
- Zon, G., & Stec, W. J. (1991) in *Phosphorothioate Oligonucleotide* (F., E., Ed.) pp 87–108, IRL Press, New York.